

# Global warming signature in observed winter precipitation in Northwestern Europe?

Torben Schmith\*

Danish Meteorological Institute, Lyngbyvej 100, 2100 København Ø, Denmark

**ABSTRACT:** For 40 precipitation series in Northwestern Europe covering the period 1900–1990, the question whether variability of winter (October to March) precipitation on all time scales longer than years can be explained by changes in circulation is investigated. This is done, for each time series, by applying a linear statistical method (multi-regression) linking the winter precipitation to the coefficients of the leading 5 principal components (PCs) of the winter mean sea level pressure. Having determined the coefficients, the corresponding hindcasted time series is obtained by applying the model. The interannual variability of winter precipitation is linked to circulation. This has been quantified by the multiple-correlation coefficient between the time series of observed and hindcasted values. Independence between these 2 time series is required for the validation to be meaningful. This is obtained by applying a cross-validation technique. The multiple-correlation coefficient is the largest in the Western Norway region. A comparison is also made between the performance of this standard model and a 'reduced' model based on the link between precipitation and the North Atlantic Oscillation (NAO) index only. This comparison shows that the performance is significantly larger using 5 PCs than using 1 PC (the NAO). In contrast, the lowest frequencies are not related to changes in the circulation. This shows up as a systematic positive trend in the difference between the observed and hindcasted precipitation for the majority of series. A Monte Carlo test reveals that this result is unlikely to have occurred by chance. This is interpreted as a change in the physics of the climate system, due to enhanced greenhouse forcing, to changes in sea surface temperatures in connection with some very low frequency mode, or to changes in land use enhancing the hydrological cycle.

**KEY WORDS:** Global warming · Climate change detection · Precipitation · Europe · Hindcast

*Resale or republication not permitted without written consent of the publisher*

## 1. INTRODUCTION

Precipitation in mid-latitudes mainly occurs in connection with the migrating synoptic disturbances (lows). Therefore, most precipitation in the northern hemisphere occurs in the 2 characteristic average storm tracks which are found over the North Atlantic and the North Pacific, respectively, and are most distinct during winter. The position of these average storm tracks varies from winter to winter, and these variations are statistically related to variations in the

winter mean circulation (Lau 1988, Rogers 1997). Since precipitation is closely related to synoptic activity, we expect variations in winter precipitation to be related to variations in the atmospheric winter mean circulation in a similar fashion. For Northwestern Europe, this is confirmed by Hurrell (1995), who considered both historical precipitation data and integrated tropospheric moisture flux divergences and found they were dependent on the state of the North Atlantic Oscillation (NAO).

Increasing the atmospheric content of greenhouse gases from the pre-industrial to the present level will directly cause a uniform warming of the lower tropo-

\*E-mail: ts@dmi.dk

sphere. This is a generally accepted partial explanation of the increase in global mean surface temperature observed during the 20th century. Other causes of the temperature rise could be climate oscillations involving the ocean on time scales of  $O(100 \text{ yr})$ .

With rising temperatures, the lower troposphere will contain more water vapour. This is due to the Clausius-Clapeyron equation, which prescribes an exponential dependence of maximum integrated water vapour content on temperature. For the extratropics (poleward of  $20^\circ$ ), this exponential dependence of *observed* precipitable water on surface temperature has been confirmed from radiosonde observations (Gaffen et al. 1992). The increasing water content has a direct radiative effect ('water vapour feedback'). In addition, one would also expect that cloud formation and therefore precipitation is favoured in a warmer climate.

The climate system is complicated, is non-linear and has a number of feedback mechanisms. Forcing this system with increased amounts of tropospheric greenhouse gases may well result in changes in the preferred circulation patterns. Ulbrich & Christoph (1999) in a general circulation model (GCM) experiment demonstrated this for the NAO, and Shindell et al. (1999) and Fyfe et al. (1999) obtained similar results for the closely related Arctic oscillation. Such changes in the circulation, induced by external forcing, are principally equivalent to naturally occurring variability in the mean circulation and therefore imply a change in the precipitation pattern.

Therefore, precipitation changes in mid-latitudes in a greenhouse-enhanced climate may come about for 2 reasons, namely *directly* from increased water content of the troposphere and *indirectly* through induced circulation changes. The indirect change in precipitation cannot be distinguished from variations in precipitation related to naturally occurring fluctuations in the mean circulation. Therefore, if the total circulation-dependent part of the precipitation can be determined for each winter and subtracted from the actually observed precipitation, this 'residual' precipitation must be equal to the *direct* precipitation change due to some changed forcing of the atmosphere, either radiative from an enhanced greenhouse effect or from changed sea surface temperature patterns.

In the present study, a method for detecting climate change along these lines will be tested. This study will be based on the observed winter (October to March) precipitation from a number of stations in Northwestern Europe over the period 1891–1990. For each station, the circulation-dependent portion of the winter precipitation totals will be identified for each year by a statistical model and subtracted from the actually observed precipitation total, that which is remaining being the 'residual' precipitation total. The hypothesis

is that this residual precipitation has increased during the years due to global warming. The scope is therefore to test this hypothesis by applying appropriate statistical tests.

Although the motivation for carrying this study out is to detect climate change, it has implications for the application of statistical 'downscaling' techniques in climate change research also, i.e. how to get information regarding changes of climate conditions on the regional or local scale from GCM scenario simulations. Using these techniques, the underlying assumption is stationarity under changed climatic conditions between the large scale (represented by the GCM) and small (regional or local) scale fields (see, e.g., von Storch et al. 1993). Therefore, it is important to test whether the assumption actually holds with observed data. The present analysis tests this for Northwestern Europe.

## 2. DATA

The monthly precipitation data used in the present analysis are taken from the North Atlantic Climatological Dataset (NACD, Frich et al. 1996). This dataset contains (in addition to 4 other climate elements: temperature, pressure, cloud cover and snow cover) monthly precipitation sums for a number of stations in Belgium, Denmark, Finland, the Faroe Islands, Greenland, Great Britain, Ireland, Iceland, Norway, The Netherlands and Sweden from the period 1890–1990. In selecting the stations to be included in the NACD, emphasis was put on selecting spatially distributed stations with long and unbroken records with few missing values. Whenever neighbouring alternative stations existed, they were examined and the 'best' ones selected.

When selecting series to be included in the NACD, great effort was also made regarding quality control and testing for 'homogeneity' of the series. A climatic time series is defined as being homogeneous when it has no spurious changes due to change in instrumentation, changes in the immediate surroundings of the station, relocation of the station, etc. (Conrad & Pollack 1962). Therefore, testing a series for homogeneity is closely connected to knowledge of the history of the station: relocations, instrumental changes etc. Such recorded pieces of information are known as *metadata*.

Series included in the NACD were statistically tested for homogeneity whenever possible. This was done according to the 'Standard Normal Homogeneity Test' (SNHT, Alexandersson 1986). Briefly, the SNHT compares series with reference series from neighbouring stations, which are assumed to be homogeneous. The

SNHT is well suited for detecting abrupt inhomogeneities or 'breaks'. The SNHT results in likely 'break points' in the series, the test statistic  $T$ , and the magnitude of the break, i.e. an adjustment factor to be applied to the values of the series on one side of the break point in order to obtain a homogeneous series. Choosing the significance level  $p$ , the null hypothesis of no break is rejected if  $T$  exceeds the  $p$  quantile  $T_p$  in the distribution of the stochastic variable  $T$ . When testing the series in NACD a break was detected if either (1) the null hypothesis is rejected at the 5% level or (2) the null hypothesis is rejected at the 10% level and the break is explainable using metadata. This application of this procedure in Norway is described in Hanssen-Bauer & Førland (1994).

Neighbouring stations which could have served as reference stations were not always available, and therefore SNHT was not possible. These stations were not excluded from the NACD. Instead, all time series were divided into the following 5 classes according to how rigorously they were tested—H: homogeneous, rigorously tested and maybe adjusted; T: tested, maybe adjusted but not perfectly homogeneous; N: not tested, but not necessarily inhomogeneous; E: environmental changes prevent climatic studies; and I: inhomogeneous series which is presently unadjustable.

In the present analysis, only series in class 'H' and covering the entire period 1900–1990 were included. If less than 5% of the values in a time series were missing, these were replaced by climatology; if not, the time series was omitted from analysis. Applying these criteria, in total 40 precipitation series were selected for the analysis. For these 40 series, the series of winter totals was formed by summing the values from the months October through March. These series were used in the entire subsequent analysis. In Table 1 details about the selected series are given, and the geographical distribution is shown in Fig. 1.

Table 1. Details of the 40 stations selected for the analysis. B: Belgium; DK: Denmark; GB: Great Britain; N: Norway; S: Sweden

No.	Country	Station name	Latitude	Longitude
1	B	Ath/Chievres	50° 38' N	3° 47' E
2	B	Leopoldsbuurg/Koersel	51° 6' N	5° 16' E
3	B	Gembloux/Ernage	50° 34' N	4° 40' E
4	B	Maredsous/Mettet	50° 17' N	4° 46' E
5	B	Rochefort	50° 11' N	5° 13' E
6	B	Thimister	50° 39' N	5° 52' E
7	B	Stavelot	50° 24' N	5° 55' E
8	B	Hives	50° 9' N	5° 35' E
9	B	Chimay	49° 59' N	4° 21' E
10	B	Chiny/Lacuisine	49° 44' N	5° 21' E
11	DK	Hammerodde Fyr	55° 18' N	14° 47' E
12	DK	Vestervig	56° 46' N	8° 19' E
13	DK	Nordby	55° 26' N	8° 24' E
14	DK	Tranebjerg	55° 51' N	10° 36' E
15	DK	Koebenhavn	55° 41' N	12° 32' E
16	GB	Lerwick	60° 8' N	1° 11' W
17	GB	Wick	58° 27' N	3° 5' W
18	GB	Stornoway	58° 13' N	6° 19' W
19	GB	Braemar	57° 0' N	3° 24' W
20	GB	Edinburgh	55° 55' N	3° 11' W
21	GB	Dumfries	55° 4' N	3° 36' W
22	N	Karasjok	69° 28' N	25° 31' E
23	N	Bjoernsund	69° 27' N	30° 4' E
24	N	Kraakmo	67° 48' N	15° 59' E
25	N	Oerskog	62° 29' N	6° 49' E
26	N	Skjaak	61° 54' N	8° 10' E
27	N	Lien I Selbu	63° 13' N	11° 7' E
28	N	Vetti	61° 0' N	7° 1' E
29	N	Reinli	60° 50' N	9° 30' E
30	N	Nedstrand	59° 21' N	5° 48' E
31	N	Mestad	58° 13' N	7° 54' E
32	N	Halden	59° 7' N	11° 23' E
33	N	Oslo-Blindern	59° 57' N	10° 43' E
34	S	Kalmar	56° 43' N	16° 17' E
35	S	Aalberga	58° 44' N	16° 33' E
36	S	Lisjoe	59° 42' N	16° 4' E
37	S	Uppsala	59° 51' N	17° 37' E
38	S	Falun	60° 37' N	15° 37' E
39	S	Haernoesand	62° 37' N	17° 56' E
40	S	Stensele	65° 4' N	17° 9' E

### 3. BASIC PROPERTIES OF THE WINTER TOTAL PRECIPITATION SERIES

#### 3.1. Observed trends

Initially, a trend test was performed on the 40 series of observed winter precipitation totals,  $R_t$ . Following Bloomfield & Nyckla (1992) the trend is evaluated as the slope of a straight line fitted to  $R_t$  as a function of the year  $t$ . I denote  $B_{\text{obs}}$  to be this slope divided by  $\bar{R}$  and multiplied by the length of the period (90 yr), i.e. the *relative* change over the period. Assuming serial independence between years of each series, the statistical significance of  $B_{\text{obs}}$  can be determined by a simple  $t$ -test (Essenwanger 1986), whose outcome is the significance level,  $p_{\text{obs}}$ , at which the hypothesis of zero trend must be rejected. This test was carried out for all 40 stations, and the results are given in Table 2. In

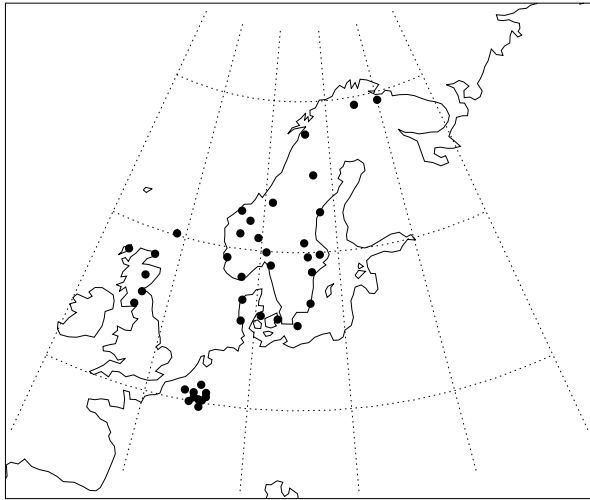


Fig. 1. Locations of the 40 precipitation stations used in this study (large solid circles)

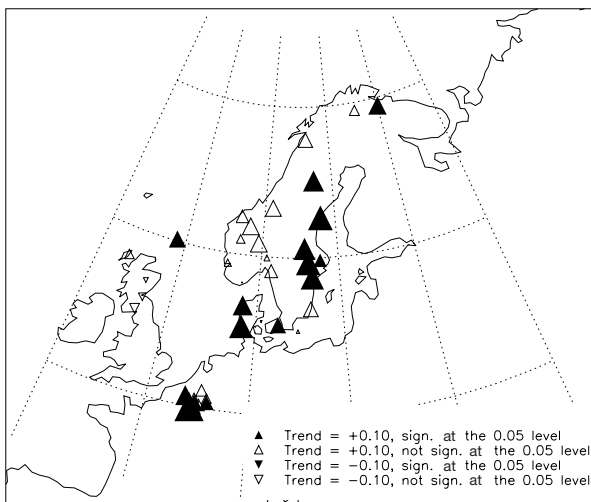


Fig. 2. Trends in observed winter (October to March) precipitation. The size and direction of the triangles indicate the size and direction of the trend. A solid triangle means that the trend is different from zero at the 0.05 level

Fig. 2 the results are graphically illustrated by triangles, whose size and direction indicate the size and direction of the trend. Furthermore, a solid triangle means that the trend significance level,  $p_{\text{obs}}$ , is 0.05 or less.

Almost all stations show a positive trend throughout the period. Thirteen of the 40 series are significant at the 0.05 significance level. This picture of a generally wetter climate in Northwestern Europe is in agreement with the results of Førland et al. (1996a) and with Schönwiese et al. (1994). It is interesting to note that the increase in winter precipitation in Western Nor-

way, although it amounts to 10–20%, is not significant at the 0.05 level.

### 3.2. Spatial correlations

Since precipitation on interannual time scales is linked to the atmospheric mean circulation, we can expect that spatial correlations exist. This was investigated more systematically by determining the correlation decay length,  $r_0$ . This was determined by fitting an exponential function  $\rho_{\text{spat}}(r) = \exp(-r/r_0)$  to the correlation coefficients for all pairs of stations as a function of distance  $r$ . This yielded a correlation decay length  $r_0 = 500$  km. Since the distance between the stations is often smaller, the effective number of independent series is smaller than the number of stations.

Jones et al. (1997) determined the correlation decay length for temperature and got 1900 km. *A priori* I would also expect a correlation decay length larger for temperature than for precipitation, since temperature is an air mass property and precipitation is connected to differences in air mass properties.

## 4. DETERMINING THE CIRCULATION DEPENDENT PART OF THE TOTAL WINTER PRECIPITATION

Following the strategy presented in Section 1, I will identify the part of the winter precipitation which depends on the winter mean circulation. This will then be removed subsequently from the observed precipitation. The 'residual' precipitation thus obtained will be analysed to reveal whether it is random noise or contains any systematic trend signal.

A statistical model will be developed for each station. In this model, the winter precipitation total (the predictand) will be linked to relevant circulation parameters (predictors) on an annual basis. The outcome of this model will be an annual series of winter precipitation depending on circulation. I will name it the 'hindcasted' precipitation. The observed less the hindcasted precipitation is the residual precipitation.

### 4.1. The model

To hindcast the winter precipitation sum from the winter mean mean sea level (MSL) circulation, a multilinear regression model was applied to each precipitation time series ( $R_t$ ) separately.

The predictors in the model are obtained from the October to March average of the mean sea level pressure (MSLP) fields over the area 30°N–80°N, 100°W–40°E. The MSLP data were obtained from

NCAR as their ds010.1. These data are given on a  $5^\circ \times 5^\circ$  grid for the period 1899 to the present day and have been extensively investigated, as described in Trenberth & Paolino (1980). A principal component analysis was performed on the winter mean MSLP field, and the leading 5 PC scores,  $\alpha_t^{(i)}$ ,  $i = 1, \dots, 5$  were used as predictors in the hindcast model. The 5 leading PCs explain almost 80% of the variance of the winter mean MSLP field, and keeping more PCs added only an insignificant portion of variance explained.

Mathematically the model is written as:

$$R_t = \bar{R} + \sum_{i=1}^5 b_i \alpha_t^{(i)} + R_{\text{res},t}$$

The coefficients  $b_i$  are determined by the usual formulas for multi-linear regression. Once these coefficients are known, the hindcasted time series can be calculated as:

$$R_{t,\text{hind}} = \bar{R} + \sum_{i=1}^5 b_i \alpha_t^{(i)}$$

which is the best (linear) guess for winter precipitation if it were entirely determined by the circulation. Subsequently, the residual time series is determined. The whole methodology is similar to the one described in Schmith et al. (1998). As an example, the observed and hindcasted time series for the station Nordby (Denmark) are shown in Fig. 3.

Table 2. Trends in the observed winter precipitation totals (October to March). Relative increase over the period 1900–1990 ( $B_{\text{obs}}$ ) and its significance level ( $p_{\text{obs}}$ ), based on a  $t$ -test

No.	Country	Station name	$B_{\text{obs}}$	$p_{\text{obs}}$
1	B	Ath/Chievres	0.239	0.010
2	B	Leopoldsbuurg/Koersel	0.136	0.090
3	B	Gembloux/Ernage	0.112	0.169
4	B	Maredsous/Mettet	0.201	0.017
5	B	Rochefort	0.138	0.097
6	B	Thimister	0.114	0.144
7	B	Stavelot	0.178	0.035
8	B	Hives	0.036	0.679
9	B	Chimay	0.350	0.000
10	B	Chiny/Lacuisine	0.037	0.648
11	DK	Hammerodde Fyr	0.041	0.605
12	DK	Vestervig	0.240	0.003
13	DK	Nordby	0.284	0.001
14	DK	Tranebjerg	-0.024	0.772
15	DK	Koebenhavn	0.194	0.013
16	GB	Lerwick	0.205	0.000
17	GB	Wick	0.010	0.866
18	GB	Stornoway	0.113	0.071
19	GB	Braemar	-0.058	0.472
20	GB	Edinburgh	-0.092	0.257
21	GB	Dumfries	-0.116	0.108
22	N	Karasjok	0.120	0.145
23	N	Bjoernsund	0.219	0.008
24	N	Kraakmo	0.171	0.134
25	N	Oerskog	0.151	0.107
26	N	Skjaak	0.199	0.103
27	N	Lien I Selbu	0.189	0.051
28	N	Vetti	0.102	0.440
29	N	Reinli	0.200	0.088
30	N	Nedstrand	0.086	0.313
31	N	Mestad	0.011	0.915
32	N	Halden	0.155	0.130
33	N	Oslo-Blindern	0.070	0.534
34	S	Kalmar	0.176	0.089
35	S	Aalberga	0.279	0.007
36	S	Lisjoe	0.293	0.003
37	S	Uppsala	0.161	0.046
38	S	Falun	0.265	0.005
39	S	Haernoessand	0.296	0.006
40	S	Stensele	0.251	0.002

## 4.2. Validation

The multiple correlation coefficient between observed and hindcasted time series cannot directly be regarded as a measure of model. To obtain a validation of the model based on independent data, we use a cross validation procedure as follows: each year in the period was hindcasted with a special version of the model, where data from the actual and the 5 neighbouring years (11 yr in total) were omitted in the fitting procedure to find the coefficients. In this way we get a time series of hindcasted values based on independent data. The multiple correlation coefficient,  $\rho$ , between this and the observed time series can be regarded as a measure of the quality of the model.

This multiple correlation coefficient between observed and hindcasted values, based on the cross validation with an 11 yr window,  $\rho$ , is shown in Table 3. together with its significance level based on a  $t$ -test,  $p_p$ . For all stations,  $\rho$  is significantly different from zero at a level below 0.05. The performance of the model, as measured by  $\rho$ , is illustrated in Fig. 4, where the size of the solid circles is proportional to  $\rho$  for the particular station. The model performs best in Western Scandinavia and Scotland.

I made a comparison between standard hindcasting model, based on 5 PCs, and a *reduced* model based on 1 PC only (the NAO index). The

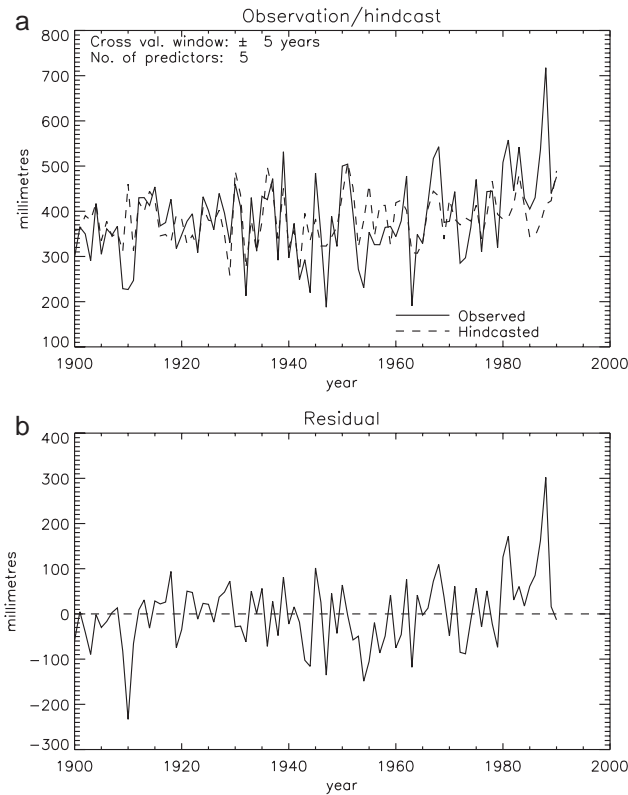


Fig. 3. (a) Observed and hindcasted winter precipitation anomaly 1899–1995 for the station Nordby (Denmark). The hindcasted values are obtained by a cross validation technique. In this application a cross validation window length of 11 yr is used. (b) Corresponding residual (observed less hindcasted) values

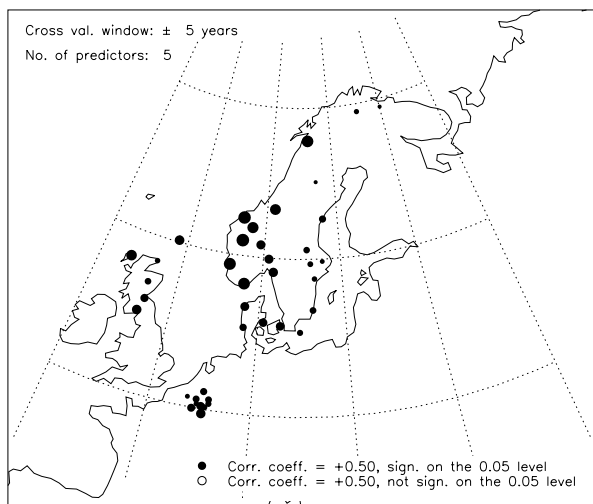


Fig. 4. Results from validation hindcast of winter precipitation anomaly of 38 NACD stations, 1900–1990. A window of 11 yr was used in the cross validation procedure. The size of the solid circles is proportional to the multiple correlation coefficient between the observed and hindcasted time series

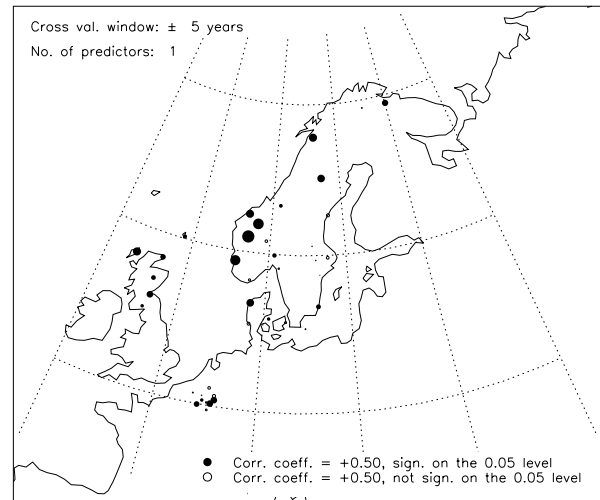


Fig. 5. As for Fig. 4, but for the *reduced* model with only 1 principal component as the predictor

reduced model corresponds to the work of Hurrell & van Loon (1997) on correlation of winter precipitation with the NAO index. The performance of the reduced model, in terms of  $\rho$  and  $p_\rho$  is given in Table 3. and graphically illustrated in Fig. 5. By comparing the relevant columns of Table 3 or by comparing Figs. 4 & 5, it appears that  $\rho$  is generally smaller for the reduced model. Choosing a significance level of 0.05,  $\rho$  obtained with the standard model is significantly different from zero for all stations. Using the reduced model,  $\rho$  for only 19 out of 40 stations is significantly different from zero, and these 19 stations are all in Norway and Northern Great Britain. This means that the NAO index is not the 'best' index to describe winter precipitation at a particular station. In fact, for each station, our standard model finds the 'optimal' circulation index to describe the winter precipitation total.

### 5. ANALYSIS OF RESIDUALS

After having determined the circulation-dependent component of the winter precipitation sum for each station by the hindcast method described in the previous section, the residual time series was calculated from each station by subtracting the hindcasted from the observed time series.

In order to determine the residual trend for each station, I let  $B_{res}$  denote the *relative* change in residual precipitation over the period 1900–1990 (calculated in analogy to  $B_{res}$ ) and determined the significance level,  $p_{res}$ , at which the hypothesis of zero residual trend must be rejected. This is quite analogous to the analysis in Section 3.1.

Table 3. Results from validation hindcast (see text for description). Shown is the correlation coefficient between observed and hindcasted series and its significance level, based on a *t*-test, both for the standard model based on 5 principal components (PCs) and for the reduced model based on 1 PC

No.	Country	Station name	Standard model (5 PCs)		Reduced model (1 PC)	
			$\rho$	$P_\rho$	$\rho$	$P_\rho$
1	B	Ath/Chievres	0.295	0.005	-0.056	0.596
2	B	Leopoldsburg/Koersel	0.432	0.000	-0.157	0.136
3	B	Gembloux/Ernage	0.421	0.000	-0.032	0.762
4	B	Maredsous/Mettet	0.329	0.001	-0.208	0.048
5	B	Rochefort	0.507	0.000	-0.083	0.434
6	B	Thimister	0.412	0.000	-0.191	0.070
7	B	Stavelot	0.371	0.000	-0.400	0.000
8	B	Hives	0.361	0.000	-0.398	0.000
9	B	Chimay	0.482	0.000	-0.343	0.001
10	B	Chiny/Lacuisine	0.569	0.000	-0.105	0.321
11	DK	Hammerodde Fyr	0.371	0.000	0.052	0.628
12	DK	Vestervig	0.537	0.000	-0.465	0.000
13	DK	Nordby	0.442	0.000	-0.175	0.097
14	DK	Tranebjerg	0.508	0.000	0.206	0.050
15	DK	Koebenhavn	0.517	0.000	-0.122	0.251
16	GB	Lerwick	0.579	0.000	0.249	0.017
17	GB	Wick	0.329	0.001	-0.329	0.001
18	GB	Stornoway	0.638	0.000	0.490	0.000
19	GB	Braemar	0.398	0.000	-0.283	0.007
20	GB	Edinburgh	0.494	0.000	-0.400	0.000
21	GB	Dumfries	0.575	0.000	-0.210	0.046
22	N	Karasjok	0.315	0.002	0.049	0.642
23	N	Bjoernsund	0.246	0.019	-0.380	0.000
24	N	Kraakmo	0.699	0.000	0.489	0.000
25	N	Oerskog	0.750	0.000	0.484	0.000
26	N	Skjaak	0.670	0.000	0.641	0.000
27	N	Lien I Selbu	0.653	0.000	0.226	0.031
28	N	Vetti	0.757	0.000	0.735	0.000
29	N	Reinli	0.548	0.000	0.155	0.143
30	N	Nedstrand	0.722	0.000	0.612	0.000
31	N	Mestad	0.705	0.000	-0.128	0.228
32	N	Halden	0.564	0.000	0.090	0.396
33	N	Oslo-Blindern	0.544	0.000	-0.263	0.012
34	S	Kalmar	0.406	0.000	0.291	0.005
35	S	Aalberga	0.330	0.001	0.009	0.933
36	S	Lisjoe	0.351	0.001	-0.032	0.765
37	S	Uppsala	0.292	0.005	-0.164	0.119
38	S	Falun	0.396	0.000	0.029	0.784
39	S	Haernoessand	0.433	0.000	0.187	0.076
40	S	Stensele	0.244	0.020	-0.458	0.000

Results from this analysis are given in Table 4 and graphically illustrated in Fig. 6. The residual trends are positive for 37 of the 40 stations. For 9 stations, the hypothesis of zero residual trend must be rejected at the 0.05 level.

Looking at the geographical distribution of the residual trend, values seem to be smallest in Western Norway, which is rich in precipitation. It is also the case that in this region the largest part of the precipitation variability is determined by circulation.

Most stations have a positive trend in the residuals, although it is significant at the 0.05 level for 9 stations only. How likely is it to obtain such a result by chance? This question is not straightforward to answer since spatial correlations exist between stations series (and also between their residuals). This hampers the application of standard statistical tests, because the data do not correspond to 40 independent series.

To overcome these problems, I therefore resorted to a Monte Carlo test designed as follows: for each reali-

sation, the years 1900–1990 are reordered randomly and then *all* residual series are reordered according to that list of years. In this way a random series without any systematic trend but with an identical spatial correlation pattern. The number of these series with positive trends is a stochastic variable whose statistical properties can be determined by carrying out this procedure many times. I chose 10 000 realisations, which by experimentation gives robust statistical evidence. It turns out that the probability of the situation with 37 or more stations with positive trends occurring in these artificial series with only random trends is smaller than 0.003. From this I conclude that the observed trend in the residuals spatially distributed over Northwestern

Europe is most likely due to some physical changes in the climate system during the 20th century.

## 6. DISCUSSION

In this section, I will discuss selected items related to the methodology I have used in my analysis.

### 6.1. Causes for the observed residual trend pattern

This study was motivated by the expectation that the rising lower tropospheric temperatures will lead to increased water vapour content in the lower troposphere. It was further mentioned that a rise in lower tropospheric temperatures could either have its origin in the enhanced greenhouse effect or low frequency natural variability of the climate system. It is interesting that Werner & von Storch (1993) found residual trends for the Northwestern European *temperature* with a methodology quite similar to mine.

Could the reason for the increased residual winter precipitation be changes in land use? Such changes may effect both the potential evapotranspiration and the vertical Ekman pumping due to friction. While the first effect is negligible during winter (since the evapotranspiration itself is negligible), the second may affect all seasons. The literature hardly contains any work on precipitation changes due to changes in surface roughness, except Sud et al. (1988). In this work, 2 GCM experiments were carried out with July conditions, one with realistic average land roughness and one with drastically reduced roughness over land. In Northwestern Europe, the difference between the 2 experiments was not different from natural variability.

### 6.2. Apparent residual trends caused by inhomogeneity of precipitation data

Inhomogeneities in the input precipitation data will show up as trends

Table 4. Trends in the *residual* winter precipitation totals (October to March). Relative increase over the period 1900–1990 ( $B_{res}$ ) and its significance level ( $p_{res}$ ), based on a *t*-test

No.	Country	Station name	$B_{res}$	$p_{res}$
1	B	Ath/Chievres	0.182	0.027
2	B	Leopoldsbuurg/Koersel	0.141	0.039
3	B	Gembloux/Ernage	0.109	0.115
4	B	Maredsous/Mettet	0.173	0.020
5	B	Rochefort	0.141	0.030
6	B	Thimister	0.096	0.148
7	B	Stavelot	0.152	0.038
8	B	Hives	0.034	0.651
9	B	Chimay	0.206	0.006
10	B	Chiny/Lacuisine	0.074	0.228
11	DK	Hammerodde Fyr	0.024	0.731
12	DK	Vestervig	0.135	0.033
13	DK	Nordby	0.190	0.008
14	DK	Tranebjerg	-0.030	0.655
15	DK	Koebenhavn	0.090	0.155
16	GB	Lerwick	0.061	0.141
17	GB	Wick	0.008	0.875
18	GB	Stornoway	0.061	0.156
19	GB	Braemar	0.072	0.286
20	GB	Edinburgh	0.028	0.670
21	GB	Dumfries	-0.042	0.442
22	N	Karasjok	0.001	0.985
23	N	Bjoernsund	0.127	0.091
24	N	Kraakmo	0.039	0.598
25	N	Oerskog	0.036	0.526
26	N	Skjaak	0.071	0.411
27	N	Lien I Selbu	0.072	0.302
28	N	Vetti	0.059	0.467
29	N	Reinli	0.059	0.524
30	N	Nedstrand	0.017	0.754
31	N	Mestad	-0.035	0.601
32	N	Halden	0.067	0.402
33	N	Oslo-Blindern	0.004	0.960
34	S	Kalmar	0.103	0.248
35	S	Aalberga	0.184	0.048
36	S	Lisjoe	0.134	0.128
37	S	Uppsala	0.076	0.311
38	S	Falun	0.117	0.156
39	S	Haernoessand	0.122	0.190
40	S	Stensele	0.124	0.104

in the residuals. Therefore, a further discussion of the homogeneity of these data is needed.

Even though great effort has been put into making the precipitation data free of such inhomogeneities, they cannot be entirely excluded. This is particularly true for inhomogeneities occurring concurrently at several neighbouring stations, since these are hard to find using the SNHT. There are 2 such types of inhomogeneities: (1) Due to the general air temperature rise, the ratio between solid and liquid precipitation decreases. Since solid precipitation is caught less efficiently by the rain gauge than wet precipitation, this means that the rain gauges will gradually catch a larger and larger fraction of the 'true' precipitation. (2) Wind shields have been installed on gauges; however, this was performed at different times in the different countries. This will also mean systematically more effective rain gauges.

For evaluating the implications, I used an empirical correction model for precipitation (Førland et al. 1996b). The details are given in Appendix 1. The outcome of these calculations is that (1) could account for a 1% increase while (2) could account for an 8% increase.

By comparing this value with values from Table 4, (1) is too small to contribute significantly, while (2) could account in principle for many of the residual trends observed. On the other hand, introduction of shielded gauges is an intended action, which is supposed to be well documented in the station histories and therefore will be identified as significant by the SNHT more easily. In an investigation of 165 Norwe-

gian precipitation series of 75 yr or more, Hanssen-Bauer & Førland (1994) discussed the detection of this type of inhomogeneity. Using a network of gauges in which no wind shield had been installed as reference stations, they were able to detect most of the serious inhomogeneities caused by the installation of windshields. However, when using an 'arbitrary' network of reference stations, they were able to detect only 30 to 40% of such inhomogeneities. This points to the essential requirement of having good station history files to supplement the SNHT. Since good-quality metadata are one of the criteria for including a time series into the NACD, I have reasons to believe that most of the (2) inhomogeneities have been detected and adjusted properly. One further reason is that wind shields have been installed in different periods in neighbouring countries, which also increases the possibility of finding homogeneous reference stations.

The most frequent type of inhomogeneity in the study by Hanssen-Bauer & Førland (1994) was that caused by relocation of the gauge. I assume this to cause both an increase and a decrease in gauge efficiency, so for a sufficiently large area this will cause no systematic disturbance of an analysis such as mine.

### 6.3. Choice of predictors

Ideally, predictors representing the 3-dimensional large-scale height field of the atmosphere should be used. Since upper-air observations exist since the late 1940s only, this demand should be weighed against the wish to carry the investigation out over as long a period as possible, which is only limited by the length of precipitation records. Therefore, I chose to base the predictors on surface pressure only. An argument for doing so is that the leading modes of interannual variability in the North Atlantic area appear to be vertically coherent (Wallace & Gutzler 1980). Therefore, the upper-air fields contain only little extra information on these temporal and spatial scales. This is also the background for the success of the NAO index in historical climate research.

When choosing predictors representing only 1 layer of the atmosphere, there is one potentially important aspect of the atmospheric structure missing—the possible systematic trend in the static stability of the atmosphere. A greenhouse-enhanced atmosphere will be less stable at mid-latitudes and this may influence the average synoptic activity and therefore the precipitation. This question was investigated for the Northeast Atlantic region by Schmith et al. (1998), who found no systematic changes in the synoptic activity which could not be explained by variations in the MSL circulation. I therefore have strong reasons to believe

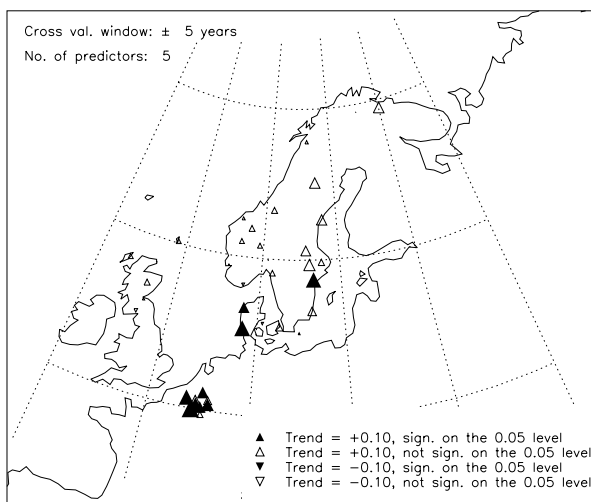


Fig. 6. Trend in residual (= observed less hindcasted) winter precipitation. The size and direction of the triangles indicate the size and direction of the trend. A solid triangle means that the trend is different from zero at the 0.05 level

that systematic changes in the vertical stability cause the residual precipitation changes through changes in the synoptic activity.

Finally it should be mentioned that it is tempting to verify the hypothesis regarding increased water vapour content of the atmosphere by relating the residuals to historical humidity observations. However, works on historical humidity observations and their quality are hardly seen only rarely in the literature. Therefore this investigation was not carried out.

#### 6.4. Semi-empirical versus dynamical methods

The semi-empirical method used here for climate change detection is appealing because of its simplicity and cost-effectiveness. Let us discuss now in more detail the advantages and disadvantages of this method versus the conventional fingerprint detection methods based on patterns obtained from GCMs (for an explanation of the state-of-the-art methods see Barnett et al. 1999).

Barnett et al. (1998) pointed out the crucial uncertainties in the GCM-based methods, namely: (1) Uncertainty in the forcing fields. Forcing include greenhouse gases, ozone, direct and indirect aerosol effects. However, not all details of these forcings are known. (2) Incorrect response of the GCM to the specified forcing. (3) Incorrect representation of internal climate variability in the GCM. (4) Errors in the observations. To these we may add: (5) Uncertainties due to the cut-off of small spatial scales in the GCM fields and no such cut-off in observed data.

It is revealing to consider whether the present method represents any improvements to the above-mentioned points. As regards point (1), my model does not have any parameterisation of the different forcings. This has been done in a statistical model for greenhouse-gas concentrations (Tol & de Vos 1998). Incorporating aerosols in statistical models is probably very difficult, if not impossible, because aerosols are not well mixed into the atmosphere and factors such as spatial distribution of sources and advection and dispersion therefore become important. The GCM-based methods certainly have an advantage in being able to model these effects, at least to a certain extent.

Points (2) and (3) are interrelated, since a part of the greenhouse-gas response coincides with the modes of natural variability. In fact, my model works by isolating that part from the detection. Therefore my model resembles what is usually called an 'optimum' detection method, where one projects observed patterns onto the part of the greenhouse response pattern from the GCM experiment, which is orthogonal to the major natural variability patterns. Our statistical model does

not have systematic errors, but does have errors due to sampling problems. In the present case, the model is trained on 90 yr of data, so variability up to the decadal time scale can be supposed to be correctly represented. In the GCM-based methods, there can be systematic errors but many coupled GCM runs have a length of up to 1000 yr, and therefore variability up to the centennial time scale is represented.

Regarding point (4), the lack of high-quality observations of good temporal and spatial (preferably global) coverage is an equally serious obstacle to both methods. For precipitation data, this problem is even more serious than for temperature.

Regarding point (5), the patterns used for climate change detection are the output from GCM experiments with T42 resolution. This meant that spatial scales smaller than approximately 300 km are not resolved. Therefore, direct comparison with observations is not possible. This is particularly true for the precipitation field in mountainous regions such as Scandinavia. The usual way to overcome this is to use a gridded data set, i.e. average the small scales out in the observed data. The model used here offers an alternative way by using the observed data from the 'local scale' directly in order to detect climate change.

## 7. SUMMARY

I fitted a semi-empirical hindcast model, using the winter mean MSL pressure field as the predictor, to observed winter precipitation sums for a number of stations in Northwestern Europe. This model can explain a significant part of the interannual variability. The model performs significantly better than a reduced model using only the NAO index as the predictor.

When the precipitation which is hindcasted by this model is subtracted from the observed precipitation sum, one obtains the 'residual' precipitation. A statistical test reveals that this residual signal is different from random noise, but for most of the series contains a systematic positive trend throughout the 20th century.

This signal could be interpreted as climate change, due either to enhanced greenhouse forcing or to very low frequency variability of the climate system.

*Acknowledgements.* This study was funded by the European Commission (ACCORD: contract No. ENV-4-CT97-0530) and by the Nordic Council of Ministers (REWARD: contract No. FS/HFj/X-93001). Thanks to the National Center for Atmospheric Research (NCAR), Boulder, CO, USA for providing the gridded mean sea level pressure data set. The valuable discussions with my colleagues Povl Frich, Eigil Kaas and Peter Thejll are appreciated, as is the suggestion from one of the reviewers to include a comparison between the performance of the standard and reduced hindcast models.

## Appendix 1. Apparent precipitation changes

In order to estimate the magnitude of apparent precipitation changes I used the method reported in Førland et al. (1996b). The basis of this work is the equation

$$R_{\text{true}} = k(R_{\text{measured}} + \Delta R_{\text{wetting}} + \Delta R_{\text{evaporation}})$$

linking measured and observed precipitation via the correction factor due to aerodynamic effects,  $k$ . The terms  $\Delta R_{\text{wetting}}$  and  $\Delta R_{\text{evaporation}}$  represent losses due to wetting and evaporation. The ingoing terms have been extensively investigated in field experiments for different types of gauges. The term  $k$  depends on wind speed, gauge type and precipitation characteristics, such as type (rain/sleet/snow), distribution of droplet size, etc. Simplifications must therefore be made. I use a 'simple correction model' procedure outlined for monthly precipitation values. In this model  $k$  is empirically given for the liquid and solid precipitation and for 5 different shelter classes.

As an example, take a site where the true precipitation is 500 mm, consisting of 450 mm liquid and 50 mm solid precipitation, falling on 60 precipitation days during the winter with a length of 180 d. Assume the shelter class to be equal to 3, and further wetting and evaporation losses

to be 0.1 mm case<sup>-1</sup> and 0.2 mm d<sup>-1</sup>. Using this as the 'normal' situation, we investigate the consequences of 2 scenarios, namely (1) removing the windshield on the rain-gauge and (2) decreasing the true snow fall to 25 mm and the rainfall accordingly to 475 mm.

The results of applying the model are given in Table A1. The model gives an observed precipitation of 420 mm for the 'normal' situation. For the 2 scenarios, the model gives 425 and 435 mm, i.e. increases of about 8 and 1%, respectively.

Table A1. Results of using a precipitation correction model for 3 different scenarios

Scenario	Wet	Dry	Total	Change relative to normal
Normal	379	32	410	–
Without wind shield	359	20	379	–0.08
Less snow	400	16	415	0.01

## LITERATURE CITED

- Alexandersson H (1986) A homogeneity test applied to precipitation data. *J Clim* 6:661–675
- Barnett TP, Hegerl GC, Santer B, Taylor K (1998) The potential effect of GCM uncertainties and internal atmospheric variability on anthropogenic signal detection. *J Clim* 11: 659–675
- Barnett TP, Hasselmann K, Chelliah M, Delworth T, Hegerl G, Jones P, Rasmusson E, Roeckner E, Ropelewsky C, Santer B, Tett S (1999) Detection and attribution of recent climate: a status report. *Bull Am Meteorol Soc* 80:2631–2659
- Bloomfield P, Nyckä D (1992) Climate spectra and detecting climate change. *Clim Change* 21:275–287
- Conrad V, Pollack C (1962) *Methods in climatology*. Harvard University Press, Cambridge, MA
- Essenwanger (1986) *Elements of statistical analysis*. Elsevier, Amsterdam
- Førland E, van Engelen A, Hanssen-Bauer I, Heino R, Ashcroft J, Dahlström B, Demarée G, Frich P, Jónsson T, Mietus M, Müller-Westermeier G, Pálsdóttir T, Tuomenvirta H, Vedin H (1996a) Changes in 'normal' precipitation in the North Atlantic region. *Klima Report 7/96*, The Norwegian Meteorological Institute, Oslo
- Førland E, Allerup P, Dahlström B, Elomaa E, Jónsson T, Madson H, Perälä J, Rissanen P, Vedin H, Vejen F (1996b) Manual for operational correction of Nordic precipitation data. *Klima Report 24/96*, The Norwegian Meteorological Institute, Oslo
- Frich P (co-ordinator) Alexandersson H, Ashcroft J, Dahlström B, Demarée GR, Drebs A, van Engelen AFV, Førland EJ, Hanssen-Bauer I, Heino R, Jónsson T, Jonasson K, Keegan L, Nordli PØ, Schmith T, Steffensen P, Tuomenvirta H, Tveito OE (1996) North Atlantic Climatological Dataset (NACD Version 1)—final report. Scientific Report 96–1. Danish Meteorological Institute, Copenhagen
- Fyfe JC, Boer GJ, Flato GM (1999) The Arctic and Antarctic oscillations and their projected changes under global warming. *Geophys Res Lett* 26:1601–1604
- Gaffen DJ, Williams PE, Robock A (1992) Relationships between tropospheric water vapour and surface temperatures as observed by radiosondes. *Geophys Res Lett* 19: 1839–1842
- Hanssen-Bauer I, Førland EJ (1994) Homogenizing long Norwegian precipitation series. *J Clim* 7:1001–1013
- Hurrell J (1995) Decadal trends in the North Atlantic Oscillation: regional temperatures and precipitation. *Science* 269:676–679
- Hurrell J, van Loon H (1997) Decadal variations in climate associated with the North Atlantic Oscillation. *Clim Change* 36:301–326
- Jones PD, Osborn TJ, Briffa KR (1997) Estimating sampling errors in large-scale temperature averages. *J Clim* 10: 2548–2568
- Lau NC (1988) Variability of the observed midlatitude storm tracks in relation to low-frequency changes in the circulation pattern. *J Atmos Sci* 45:2718–2743
- Rogers JC (1997) North Atlantic storm track variability and its association to the North Atlantic oscillation and climate variability of Northern Europe. *J Clim* 10:1635–1647
- Schmith T, Kaas E, Li TS (1998) Northeast Atlantic winter storminess 1875–1995 re-analysed. *Clim Dyn* 14:529–536
- Schönwiese CD, Rapp J, Fuchs T, Denhard M (1994) Observed climate trends in Europe 1891–1990. *Meteorol Z NF* 3:22–28
- Shindell DT, Miller RL, Schmidt GA, Pandolfo L (1999) Simulation of recent northern winter climate trends by greenhouse-gas forcing. *Nature* 399:452–455
- Sud YC, Shukla J, Mintz Y (1988) Influence of land surface roughness on atmospheric circulation and precipitation: a sensitivity study with a general circulation model. *J Appl Meteorol* 27:1036–1054

- 
- Tol RSJ, de Vos AF (1998) A Bayesian statistical analysis of the enhanced greenhouse effect. *Clim Change* 38: 87–112
- Trenberth KE, Paolino AD Jr (1980) The northern hemisphere sea-level pressure data set: trends, errors and discontinuities. *Mon Weather Rev* 108:855–872
- Ulbrich U, Christoph M (1999) A shift of the NAO and increasing storm track activity over Europe due to anthropogenic greenhouse gas forcing. *Clim Dyn* 15:551–559
- von Storch H, Zorita E, Cubasch U (1993) Downscaling of global climate change estimates to regional scale: an application to Iberian rainfall in wintertime. *J Clim* 6: 1161–1171
- Wallace JM, Gutzler DS (1980) Teleconnections in the geopotential height field during the Northern hemisphere winter. *Mon Weather Rev* 109:784–812
- Werner PC, von Storch H, (1993) Interannual variability of Central European mean temperature in January-February and its relation to large-scale circulation. *Clim Res* 3: 195–207

*Submitted: March 24, 2000; Accepted: September 6, 2000*

*Proofs received from author(s): March 1, 2001*